On the High Fluctuations of Received Signal Strength Measurements With BLE Signals for Contact Tracing and Proximity Detection

Laura Flueratoru, *Graduate Student Member, IEEE*, Viktoriia Shubina, *Graduate Student Member, IEEE*, Dragoş Niculescu, and Elena Simona Lohan, *Senior Member, IEEE*

***Abstract*—This paper presents a measurement-based analysis of the Received Signal Strength (RSS) of Bluetooth Low Energy (BLE) signals, under Line-of-Sight (LOS) and Non-Line-of-Sight (NLOS) scenarios, performed in tandem at two universities in Tampere, Finland, and Bucharest, Romania. We adopted the same hardware and methodology for measurements in both places, and paid particular attention to the impact of RSS on various environmental factors, such as LOS and NLOS scenarios and interference in 2.4 GHz band. In addition, we considered the receiver orientation and the different frequencies of BLE advertising channels. We show that snapshot RSS measurements typically have high variability, not easily explainable by classical path-loss models. A snapshot recording is defined here as one continuous recording at fixed device locations in a static setup. Our observations also show that aggregated RSS data (i.e., considering several snapshot measurements together) is more informative from a statistical point of view and more in agreement with current theoretical path-loss models than snapshot measurements. However, in BLE applications such as contact tracing and proximity detection, the receivers typically have access only to snapshot measurements (e.g., taken over a short duration of 10–20 minutes or less), so the accuracy of contact-tracing and proximity detection can be highly affected by RSS instabilities. In addition to presenting the measurement-based BLE RSS analysis in a comprehensive and well-documented format, our paper also emphasizes open challenges when BLE RSS is used for contact tracing, ranging, and positioning applications.**

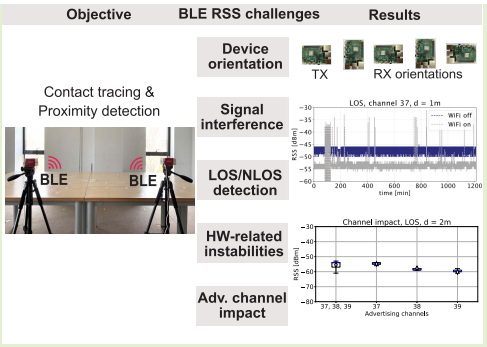

***Index Terms*—Indoor navigation, indoor radio communication, received signal strength indicator (RSSI), Bluetooth, fluctuations.**

Manuscript received March 31, 2021; revised June 27, 2021; accepted June 29, 2021. Date of publication July 8, 2021; date of current version March 14, 2022. This work was supported in part by the European Union's Horizon 2020 Research and Innovation Program through the Marie Skłodowska Curie (A-WEAR: A network for dynamic wearable applications with privacy constraints) under Grant 813278 and in part by a Grant from the Romanian National Authority for Scientific Research and Innovation (UEFISCDI) under Project PN-III-P2-2.1-PED-2019-5413. The associate editor coordinating the review of this article and approving it for publication was Prof. Stefan Knauth. *(Laura Flueratoru and Viktoriia Shubina contributed equally to this work.) (Corresponding author: Laura Flueratoru.)*

Laura Flueratoru and Viktoriia Shubina are with the Computer Science Department, Politehnica University of Bucharest, 060042 Bucharest, Romania, and also with the Electrical Engineering Unit, Tampere University, 33720 Tampere, Finland (e-mail: laura.flueratoru@uvapb.ro; viktoriia.shubina@tuni.fi).

Dragoş Niculescu is with the Computer Science Department, Politehnica University of Bucharest, 060042 Bucharest, Romania (e-mail: dragos.niculescu@upb.ro).

Elena Simona Lohan is with the Electrical Engineering Unit, Tampere University, 33720 Tampere, Finland (e-mail: elena-simona.lohan@tuni.fi).

Digital Object Identifier 10.1109/JSEN.2021.3095710

I. Introduction and Motivation

PROXIMITY-BASED applications have become increasingly popular in recent years. Estimating the distance between two devices can be used to find lost objects, to share files between nearby devices, to enable smart homes to react to owners' location, or to fight against a pandemic. In the past year, digital contact-tracing applications (shortly called apps) have received increasing attention to prevent the spread of COVID-19 and many countries have developed such digital apps. Detailed overviews of existing contact-tracing apps can be found in our previous works [1], [2] and in other recent works [3]–[7].

The most popular technologies that enable proximity-based applications are Wi-Fi, Bluetooth Low-Energy (BLE), Ultra-Wideband, and Global Navigation Satellite Systems (GNSS). BLE is the most promising candidate of them since it offers the lowest power consumption and is supported by most mobile devices and operating systems [8]. While BLE-based positioning can reach meter-level accuracy when both angle-

of-arrival (AOA) and received signal strength (RSS) information are combined [9], most consumer devices such as mobile phones and wearables are not equipped with direction-finding capabilities and they rely only on RSS measurements for proximity detection. RSS measurements from any wireless signal (BLE, Wi-Fi, cellular, etc.) are known to fluctuate due to the presence and movement of people in the signal's path [10], the presence of multipath [11], the switches between carrier frequencies of sub-channels used in the transmitted signal [11], the antenna polarization [12], the orientation of the transmitter (TX) and receiver (RX) [13], and the chipset model [14].

While there are currently many studies about the RSS variability in Wi-Fi signals, e.g., [15]–[19], most such studies focus only on one source of fluctuations or investigate the aggregated effect of multiple error sources. In contrast, this paper documents the (in)stability of the BLE RSS over time, over space (with different multipath characteristics), with different hardware, on different advertising channels, at different distances, with different device orientations, and with different type of obstructions between device pairs. We isolated these factors and evaluated their impact individually. In addition, we documented a new error source, namely the influence on Wi-Fi–BLE combo chipsets on the RSS. Based on an extensive measurement campaign, we provide recommendations that can partly mitigate BLE fluctuations caused by these factors.

We also provide open-access data that accompanies this study in order to aid future research. During the COVID-19 pandemic, open-access BLE RSS data sets have proven essential for the research community. However, most such data sets, e.g., [20]–[22], have limited documentation or do not analyze the behavior of the BLE RSS with all the aforementioned instability sources. Therefore, a more thorough investigation on BLE RSS instabilities documented by open-source data is still needed.

This paper offers a comprehensive analysis of BLE RSS instabilities, fluctuations, and challenges in BLE-based proximity detection and contact tracing. We based the analysis on two extensive measurement campaigns performed in parallel at Tampere University (TAU) in Tampere, Finland and at University Politehnica of Bucharest (UPB) in Bucharest, Romania between January–March 2021. The tandem measurements were conducted with exactly the same type of devices to eliminate the possible fluctuations coming from different hardware models as well as possible calibration issues. Our measurements will be available, upon the paper publication, in open-access at the A-WEAR research community on Zenodo.[1]

The main contributions and findings of this paper are:

- Offering an extensive measurement-based analysis of BLE RSS fluctuations and showing that current single-slope path-loss models from the literature do not capture these effects.
- Comparing snapshot (or single recording) measurements with aggregated recordings and showing that, when enough RSS data is aggregated, the statistics converge to stable models;
- Analyzing the effect of BLE advertising channels on RSS fluctuations and showing that the aggregated RSS from all BLE advertising channels has significantly higher fluctuations than on individual BLE channels. This is an important challenge in current BLE-based proximity apps, where channel information is usually not available;
- Analyzing the effect of non-line-of-sight (NLOS) propagation on the BLE RSS;
- Analyzing the effect of relative orientations between the transmitter and the receiver on the RSS;
- Analyzing the same-chip Wi-Fi interference with BLE.

[1]https://doi.org/10.5281/zenodo.4643668

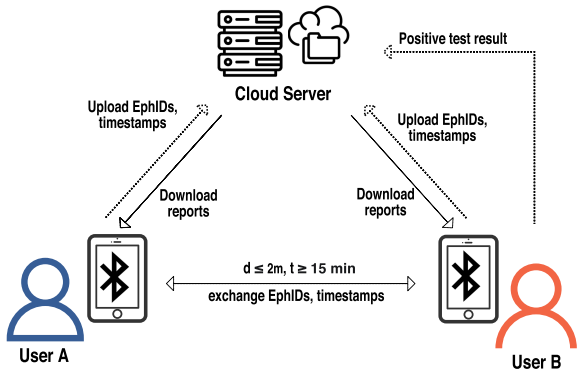

Fig. 1. An illustration of the contact-tracing chain with users *A* and *B* exchanging BLE signals at a distance of at most 2 m and interacting with the cloud server to receive the anonymized reports for crossing paths with infected users.

Based on our state-of-the-art review (Section II), we believe that these high BLE RSS fluctuations have not yet been reported and documented to their full extent in the current literature and that there are still several challenges to be overcome when dealing with snapshot BLE RSS measurements, as those used in contact-tracing and proximity detection applications. Therefore, this paper documents BLE RSS fluctuations and raises several research questions about the applicability of classical path-loss models in the line-of-sight (LOS) and NLOS propagation of BLE signals.

II. State-of-the-Art Overview

In Section II-A we provide an overview of the state-of-the-art in digital contact tracing and proximity detection apps based on BLE signals, which are increasingly relevant in our times. In Section II-B we discuss the main factors that cause BLE RSS variability and the most important studies that have investigated them. In Section II-C we summarize the findings and state the key points that differentiate our work from past research.

A. BLE-Based Contact Tracing and Proximity Detection Principles

Digital contact tracing is a particular case of proximity detection, used as an identification and follow-up solution

aiming to break the transmission chains of airborne infections within communities.

In a digital contact-tracing chain such as in Fig. 1, smartphones and wearables are commonly assigned with permanent and temporary identifiers generated by each device for privacy-preserving purposes. The server owns the complete list of the users reporting their confirmed cases of infection, which includes both permanent and ephemeral IDs. Periodically, the user devices receive anonymized data with user reports of confirmed test results from the server, such as the case of the user A in Fig. 1, and then locally estimate the risk of having been exposed to the infection.

A device equipped with a BLE chipset starts to log the ephemeral IDs and timestamps of other users when these are nearby (within a distance d) for a certain time window (e.g., typical thresholds used in many apps nowadays are 15 min time widow and $d = 2$ m distance, which is currently deemed a safe distance). The infection risk is computed based on the time spent in proximity with a confirmed case.

By nature, BLE signals are susceptible to the environment and therefore require calibration and averaging. When the range is estimated with a certain error, there is a higher risk of generating false positives, when a user appears to be closer than in reality, or false negatives, when the actual distance is less than the estimated one. These errors could also appear if a wall or a door blocks the space between the devices, leading to NLOS propagation, when in fact the infection risk is low. Therefore, it is crucial to accurately estimate the range between two users. When the estimation fully relies on BLE RSS measurements, it is therefore important to understand the various causes of BLE RSS fluctuations.

B. Related Studies on BLE RSS Variability

BLE was primarily designed for communication purposes and its use as a ranging technology has appeared only recently. As any wireless signal, BLE signals are susceptible to environment dynamics such as multipath, signal scattering, shadowing, refraction, or attenuation. In addition, the difficulty of evaluating the exact distance between two persons might be exacerbated by noisy measurements, faulty BLE chipsets, low transmit power, low received signal strength, or infrequent scanning intervals [2].

One of the key challenges of digital contact tracing, which is the scope of on-going research, is the high false positive rate. This occurred, for example, when experts from The Alan Turing Institute used the GAEN system to build the National Health Service (NHS) COVID-19 app [23]. The authors reported a problem of high false positive rates in detecting distances between users staying apart from 2 to 4 m; in other words, 2 m distance proved to be a reliable threshold both for epidemiological safety measures and for BLE performance specifications. Another critical goal for contact tracing is accurate LOS and NLOS detection, yet many factors are still unknown regarding BLE signal propagation. In the following, we outline some of the most important challenges in proximity detection based on BLE RSS and the state-of-the-art concerning them.

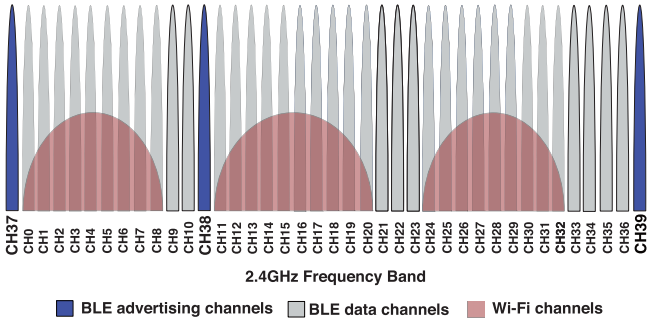

Fig. 2. An illustration of the 2.4GHz ISM band channels. Advertising channels 37, 38, and 39 are scattered deliberately to avoid interference with Wi-Fi.

1) Advertising on Different Carrier Frequencies: BLE uses 40 radio frequency (RF) channels, 2 MHz wide each and assigned with a unique index illustrated in Fig. 2. BLE channels are divided into two groups: advertisement channels (indexed 37, 38, and 39) and data channels (indexed from 0 to 36). In BLE, the three advertisement channels indexed 37, 38, and 39 with center frequencies at 2.402, 2.426, and 2.48 GHz, respectively, are scattered over the 2.4 GHz band to avoid interference with other devices operating in the Industrial, Scientific, and Medical (ISM) band. Based on the analysis and modeling of these advertising channels in [24], channel 39 was deemed the most reliable, since it is further away from the center frequency of a main Wi-Fi channel, whereas channels 37 and 38 overlap with one, respectively two Wi-Fi channels.

The impact of advertising channels on the RSS is twofold. First, according to path-loss models, the RSS is inversely proportional to the squared carrier frequency. Second, embedded antennas usually do not have a flat response over the entire bandwidth, resulting in different gains depending on the frequency [25]. The difference between RSS values acquired at the same location on different channels was found to be as high as 15 dB in [11] or almost 6 dB in [25], therefore decreasing the RSS-based ranging accuracy.

Knowing the channel on which a beacon was transmitted can improve distance estimates [11], [26], but this information is often obfuscated by the driver at the receiver, unless the transmitter explicitly includes this information in the beacon's payload (which is rarely done). As a result, most receivers cannot recover the advertising channel index on which a beacon was transmitted. Smartphones usually switch between all three advertising channels, resulting in RSS fluctuations. In [11], the authors proposed a method for identifying the advertising channel at the receiver by exploiting the pattern with which some smartphone models switch between the advertising channels.

2) Multipath Propagation: Multipath propagation causes radio signals to arrive at the receiving antenna via multiple paths due to reflection, refraction, or scattering [37]. Signal components arriving through different paths can add up constructively or destructively, the latter resulting in multipath fading. The channel-dependent multipath fading of BLE

TABLE I
OVERVIEW OF STATE-OF-THE-ART: MEASUREMENT-BASED BLE RSS STUDIES AND DATASETS

Reference	**Year**	**BLE RSS provided in open access?**	**Measurement devices (transmitter side)**	**Studied effects related to RSS**
[27]	2015	No	StickNFind (SNF) beacons	RSS fluctuations based on transmitter–receiver (TX–RX) distance.
[28]	2016	No	RN4020 PPDB board with RN4020 BLE chipsets	RSS fluctuations based on TX–RX distance and BLE channels 1, 10, 20, and 30 (non-advertising channels).
[29]	2018	No	iBKS105 BLE beacons	RSS fluctuations based on multiple carrier frequencies on advertising channels (i.e., channels 37,38, and 39); orientation effects are also discussed but directly in the context of positioning, not as effects on RSS.
[24]	2018	No	nRF52840 wireless System on Chip (SoC)	Advertising channels characterization in the BLE standard.
[13]	2018	No	A smartphone and Estimotes BLE beacons	RSS fluctuations based on different TX power levels, device orientations, advertising intervals, LOS/NLOS cases, density of the devices.
[30]	2018	Yes	Gimbal SEries 10 BLE iBeacons	One-month measurement campaign generated from 10 BLE beacons transmitting signal and carried by people inside a university building, reporting a realistic scenario.
[31]	2019	No	Raspberry Pi 3 (Model B)	RSS fluctuations based on receiver orientation, transmit power, and TX–RX distance.
[32]	2019	Yes	Accent Systems' IBKS 105 with Nordic nRF51822 BLE chipset	None (database was used to study BLE-based positioning, but RSS fluctuations are not studied separately).
[11]	2020	No	8 Android mobile phones and one iPhone 6	RSS fluctuations based on multiple carrier frequencies on advertising channels and on the TX–RX distance.
[33]	2020	Yes	Nokia 8.1 with Android 10, HTC M9 with Android 7.0 Nougat	RSS fluctuations based on the TX–RX distance with respect to various transmitter orientations/placements on the body.
[34]	2020	No	3 Android mobile phone models	RSS fluctuations based on the TX–RX distance, on the presence of human bodies (and their orientation) around TX and RX devices, on a NLOS scenario due to wall presence, and on mobility of persons carrying the mobile phones.
[35]	2020	Yes	Raspberry Pi 3 (Model B)	Three scenarios of different room sizes and with the use of Zigbee, BLE, and WiFi are documented. The authors reported different techniques for precise and accurate location estimates, where K-Nearest Neighbor (KNN) was chosen as an optimal solution.
[20]	2020	Yes	iPhone 10, Ubertooth One, nRF52 eval board	RSSI dataset collected in different environments, with various device orientations and body placements.
[21]	2020	Yes	Raspberry Pi Zero W, Raspberry Pi 3, and Raspberry Pi 4	RSSI data collected at different distances via GAEN.
[22]	2020	Yes	Samsung Galaxy S7, iPhone 7, iPhone 11 Pro	Data set of measurements collected in the university environment, interchanging device pairs used as TX and RX.
[36]	2021	Yes	Android smartphones: Nokia 8.1 with Android 10, HTC M9 with Android 7.0 Nougat	Report of RSSI fluctuations with different device placements on human bodies; described the effect of window size on the accuracy of the estimates.
This article	-	Yes	Raspberry Pi 4 (Model B+, Cypress CYW43455)	RSS fluctuations based on LOS/NLOS scenarios, NLOS cases with different obstacles, receiver orientations, multiple carrier frequencies on BLE advertising channels, on-chip BLE and Wi-Fi interference in 2.4GHz band, hardware instabilities, and the TX–RX distance; also the test–retest reliability of measurements is addressed here.

signals was studied in [25]. Channels experience deep fades at different locations due to their different center frequencies. The effect of multipath fading was eliminated in a training phase by averaging the RSS in a window. In that case, window sizes of 0.5 s to 2 s mitigate fading effects for walking speed at a BLE packet reception rate of 25 Hz. However, in practice, such a high advertising rate is uncommon as it increases the energy consumption, so observation windows need to be longer to mitigate multipath fading.

The authors in [28] noticed RSS fluctuations on the order of 6 dB at the same TX–RX distance due to the presence of multipath and Wi-Fi interference. The authors in [29] also noticed fluctuations as large as 25 dBm over short periods of time, in particular for channels 38 and 39 due to channel-dependent fast fading.

In [34], the authors studied RSS fluctuations at various TX–RX locations and noticed that the average RSS is not always decreasing with distance, as predicted by path-loss models [27], but they observed that the average RSS at 2.5 m was consistently higher than the average RSS at 2 m, also when measurements were done with different BLE transmitters. They also observed signal fluctuations as high as 20 dB at constant TX–RX locations, due to human movement around the BLE transmitters.

3) Orientation: The way people are holding their mobile devices (e.g., inside front of back pockets, in hand, inside a bag, etc.) influences the relative orientation between transmitter and receiver antennas. These orientation changes can, in turn, cause RSS fluctuations. Fluctuations of up to 30 dB between maximum and minimum RSS at constant TX-RX distances were observed in [31] when RSS data acquired with different device orientations was aggregated.

The authors in [13] found that different device orientations can affect the RSS with differences of up to 3 dB at exactly the same TX-RX distance, and that an RSS at 3 m TX-RX distance can be higher (with few dBs) than the RSS at 1 m TX-RX distance, if different receiver orientations are used.

4) Transmit Power: The RSS also depends on the transmission power, the RF front-end characteristics, and the antenna gain. Because these factors depend on the hardware or implemented firmware, the observed RSS from devices from different manufacturers can vary even when the environmental conditions are identical. This behavior was documented in [38] where, even though transmitters from different vendors had different TX powers, the RSS was within the same range. In [39] it was shown that the transmission power influences the localization accuracy and the authors proposed machine learning models to identify the individual TX power of the deployed beacons that maximize the localization accuracy.

One way to solve this issue is to compute RSS correction factors at the transmitter and the receiver [40]. The calibrated TX power can be measured for a particular model of transmitter at a known distance (e.g., 1 m for the iBeacon standard and 0 m for EddyStone) and sent in the payload of the advertising beacon. For instance, if a transmitter has a calibrated TX power of −45 dBm at 1 m, an RSS of −55 dBm will indicate that the receiver is at more than 1 m away from the transmitter, whereas for another device model −55 dB might be the calibrated TX power. Similarly, each receiver should have a correction coefficient that reflects the receiver efficiency, or with how much its RSS deviates from a reference value. Ideally, there should be a database with RSS correction factors for each mobile device. However, such a task is intractable because of the sheer number of mobile devices on the market. A 2015 report counted more than 24, 000 Android devices made by almost 1300 companies [41]. Moreover, as we will show in Section IV-C, this does not account for RSS variations between devices from the same model. To the best of the authors' knowledge, the RSS variability within devices from the same vendor has not been documented in the literature.

5) Non-Line-of-Sight Between the Devices: RF signals propagate at a different speed through the air than through obstacles such as walls, furniture, or the human body. Therefore, obstructions between the transmitter and the receiver will typically cause fluctuations in the RSS. There are several research works [26], [42], [43] that investigated the effect of shadowing on the BLE RSS with applications in proximity detection or localization. [26] proposed artificial neural network (ANN) models for detecting human-body shadowing and compensating RSS values to improve distance measurements or localization based on the BLE RSS. In the best case, the ANN can correctly detect the obstacle more than 87% of the time. The method leverages measurements acquired on *individual* channels, so knowledge of the advertising channel is also required, as well as a training phase for the ANN.

In [43], the authors proposed a NLOS detection method based on the variance of the BLE RSS. The algorithm is able to detect when a concrete wall is blocking the direct path between the transmitter and the receiver with an accuracy of 76.25% based on a fixed threshold of the RSS variance, below which the signal is classified as being acquired in NLOS. The same method could not be applied on NLOS with plasterboards, since the standard deviation was inconsistent. The effect of several obstacles (wooden door, iron door, window, hand, paper) on the BLE RSS was studied in [38]. The mean RSS values obtained with these obstructions varied between −50 dBm to −90 dBm at a TX–RX distance of 2 m. The strongest attenuation was caused when a hand covered the transmitter and when the LOS was blocked by an iron door. These results show that different NLOS obstacles can have a different impact on the RSS and that the topic should be further explored.

In [34], a NLOS case was analyzed with two types of walls between the TX and RX: a stud partition and a blockwork wall. No differences between LOS and NLOS scenarios were observed for the stud partition, while the blockwork wall introduced attenuations of up to 20 dB in the received signal strength compared to LOS case. The main conclusions in [34] are similar to the ones in our measurement-based analysis, that BLE signals have high fluctuations and their RSS does not necessarily follow classical path-loss models. Therefore, developing accurate BLE RSS-based proximity-detection methods remains a challenging topic.

Changes caused by the human body in wireless signal propagation in the 2.4 GHz band have also been documented in [44]–[46].

6) Interference in ISM Band at 2.4 GHz: As the ISM band is heavily used by many wireless systems, fluctuations in the BLE RSS are also caused by RF interference, especially coming from shared antennas between Wi-Fi and BLE modules coexisting on the same chipset (as it is the case with most mobile phones). The authors in [28] noticed RSS fluctuations on the order of 6 dB at the same TX-RX distance due to multipath fading and interferences from Wi-Fi.

The authors in [38] performed an experiment in which a BLE TX was placed directly under a Wi-Fi access point (AP) and the RSS was recorded, in turns, when the AP was on and off. When the Wi-Fi AP was on, the reception rate dropped to 75% and the RSS decreased with 10 dB in 50% of the measurements compared to the case in which the AP was turned off. We further explore this topic in Section IV-G.

C. State-of-the-Art Summary

The work in [34] can be seen as the closest to our work from the BLE RSS literature (as summarized also in Table I). However, our work focuses only on indoor scenarios in a more systematic approach, by duplicating BLE RSS measurements in two different locations (Tampere and Bucharest), by performing extensive and repetitive tests at distances relevant to contact-tracing apps (i.e., 1 to 3 m), and by investigating the effects of Wi-Fi interference and the three BLE advertising channels.

The main reason we focused on indoor scenarios is that outdoor proximity detection can be achieved with high-accuracy GNSS receivers. For indoor proximity detection, however, there are more viable candidates, out of which BLE is the most promising but also perhaps the most challenging one. In addition, in digital contact tracing apps, infectiousness levels are lower outdoors than indoors [47], [48].

Our paper offers a comprehensive survey of various causes of BLE RSS variability as well as of the related works in the literature. The state-of-the-art main studies on BLE RSS are summarized in Table I and the last row shows the contributions of this article at a glance.

Other works in similar spirit but for Wi-Fi, found variations across channels, time scales, interfaces used for 5GHz Wi-Fi [49], and across direction, device manufacturer, sampling period, presence of humans and of other radio devices [50].

For IEEE 802.15.4, that also uses 2.4GHz ISM band, but lower power, [51] finds that the main variability sources when measuring RSS are antenna orientation, hardware sample, and link asymmetry.

III. Measurement-Based BLE Data Collection

In all our experiments, we used Raspberry Pi 4 Model B devices, as illustrated in Fig. 3. The internal 2.4 GHz antenna is located in the left upper corner, next to the Cypress CYW43455 combo Wi-Fi and BLE module. The devices have a 1.5 GHz 64-bit Quad-Core Cortex-A72 CPU in the middle of the Raspberry Pi. The Gigabit Ethernet, two USB 3.0 and two USB 2.0 ports are located on the right, which might cause signal degradation in some TX–RX orientations (which will be discussed in Section IV-F). One advantage of using this hardware is that we can configure the advertising channel and payload, an option that not many open-source smartphone applications offer.

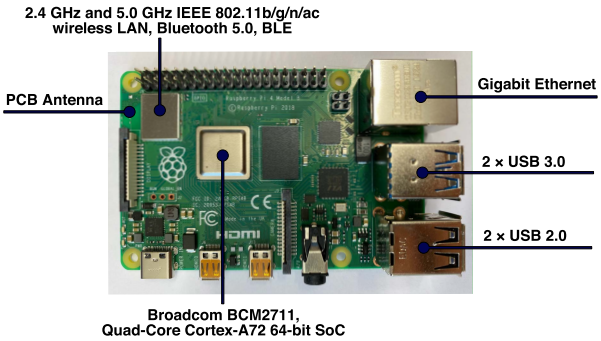

Fig. 3. Raspberry Pi 4 Model B devices are used in our experiments as TX and RX.

We acquired a database of BLE RSS measurements between devices placed at 1, 2, and 3 m in several LOS and NLOS scenarios with obstructions caused by walls (with and without a whiteboard on it), human body, plexiglass panels, and doors, shown in Fig. 4. We conducted two measurement campaigns in parallel at UPB and TAU. The different locations enabled us to compare and validate measurements acquired with the same hardware models but in different settings.

We define a *measurement* as the process of collecting data in a specific manner. Measurements can be grouped in *recordings* (or *snapshot* measurements), when data is collected continuously from a start time to an end time, in a static setup and without modifying the devices in any way, and in *scenarios* (or *aggregated* measurements), which are collections of recordings according to a pre-defined criterion. For instance, a scenario can be a collection of recordings acquired in LOS, with a TX–RX distance of 1 m, on channel 37.

We configured the transmitter to send non-connectable undirected advertisements (`ADV_NONCONN_IND`) with a period of 100 ms, which satisfies the broadcasting interval recommendation of 200 ms to 270 ms of the Bluetooth protocol for contact tracing developed by Apple and Google [52]. The same specification suggests a scanning period (at the receiver) of at least 5 min, although this is likely to vary depending on the application. For instance, in the GAEN API the scanning period was found to be between 2.5 and 4 min [53]. Since a higher scanning rate provides more RSS samples and the devices are not energy-constrained, we chose a scanning frequency of 1 Hz.

The recording time ranged from 3 minutes to 3 days. In some cases, we were interested in the stability of RSS measurements over a longer period of time, case in which the recording time spanned several days, whereas in other cases we were interested in the variability of RSS measurements at different locations with constant TX-RX distances, case in which shorter recording times of several minutes were more convenient. Fig. 4 shows examples of LOS and NLOS scenarios in which data was acquired at TAU and UPB.

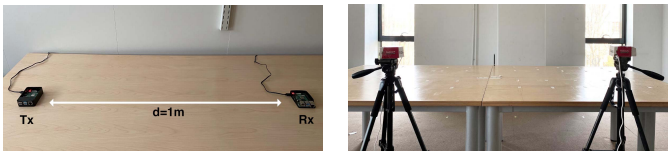

(a) LOS at TAU (b) LOS at UPB

(c) NLOS with wall at TAU (d) NLOS with wall at UPB

(e) NLOS with plexiglass at UPB (f) NLOS with human body at UPB

(g) NLOS with door at UPB (h) NLOS with wall and whiteboard at UPB

Fig. 4. The pictures of the receiver and transmitter in LOS and NLOS with wall acquired at UPB and TAU (Fig. 4a to 4d). Fig. 4e to 4h show NLOS scenarios with a plexiglass panel, human body, a door, and a wall with a whiteboard at UPB.

IV. Measurement-Based BLE RSS Characterization

This section provides an overview of the results acquired during our experiments and describes the challenges discussed in Section II-B.

In order to compare in a comprehensive manner the RSS distributions in different scenarios, throughout this section we represent the data using standardized box plots such as the one in Fig. 5, as they give information at-a-glance about the mean, median and spread of the RSS. The box shows where most of the RSS values are found, namely the data from the first quartile (Q1 or the 25^{th} percentile) to the third quartile (Q3 or the 75^{th} percentile), also known as the interquartile range (IQR). The lines extending from the box are called whiskers and cover the range from $a \triangleq Q_1 - 1.5*(Q_3 - Q_1)$ to $b \triangleq Q_3 + 1.5*(Q_3 - Q_1)$ (corresponding to Tukey's original definition of box plots). The red vertical line inside the box plot denotes the median. In some plots, we also added via a diamond marker, the mean of the data. The circle markers to the right (can also appear to the left) of the whiskers are outliers. Occasionally, the outliers or the mean value are omitted in our plots to preserve a good readability of the plot. In some cases, the RSS is stable enough that the IQR contains only the median value and therefore the box is not shown.

A. The (In)stability of BLE RSS Measurements Over Time

We first investigate the stability of BLE RSS measurements in a particular setting over time. Fig. 6 shows the boxplots

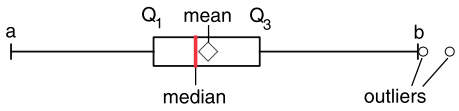

Fig. 5. Box plot used to describe and compare the RSS distribution.

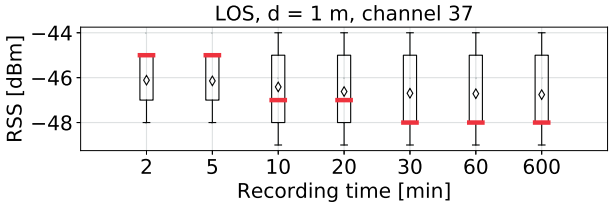

Fig. 6. The effect of the time evolution on the RSS distribution in LOS on a single channel (37), recorded at UPB.

of the BLE RSS distribution in windows of 2 min up to 10 h acquired in LOS, on channel 37, at a distance of 1 m between the transmitter and the receiver. The measurements were acquired in a locked room during the weekend, so there was no human activity around the devices during the recording. Although the median RSS changes with up to 3 dB over the course of the recording, the mean RSS varies with less than 1 dB with different window lengths.

It can be seen from Fig. 6 that, if we are interested only in the mean RSS, then a recording time of 2 min is sufficient to obtain the mean RSS that best captures the characteristics of the particular setting in which measurements are acquired. If we are also interested in the shape of the distribution, a longer recording time of at least 30 min is necessary. In general, the RSS during each snapshot recording was stable over time with the exception of some random fluctuations that sometimes appeared at the beginning of a recording and which will be discussed in Section IV-G.

B. The (In)stability of BLE RSS Measurements Over Space or Test–Retest Reliability Studies

Next, we study the stability of the BLE RSS under LOS scenarios, at a fixed distance of 1 m between the same TX–RX pair, and using only the advertising channel 37 in order to eliminate frequency-dependent fluctuations. We acquired measurements at TAU and UPB, in different rooms or with the TX and RX placed in different spots in the same room, while maintaining a distance between the two devices of 1 m. Fig. 7 compares the RSS distribution in 15 recordings when taking a fixed number of 326 random measurements from each recording (the fixed number was selected based on the minimum length among all 15 recordings).

We expected to get similar RSS measurements in different snapshot recordings, given that the multipath fading is mitigated by averaging samples over several minutes. However, even after multiple test-retest measurements performed at UPB and TAU, results (see Fig. 7) indicate fluctuations of the median RSS of up to 40 dB between snapshot recordings even though the TX–RX distance was constant. Moreover, the median RSS can vary even in the same location between two recordings taken in different days, even though results

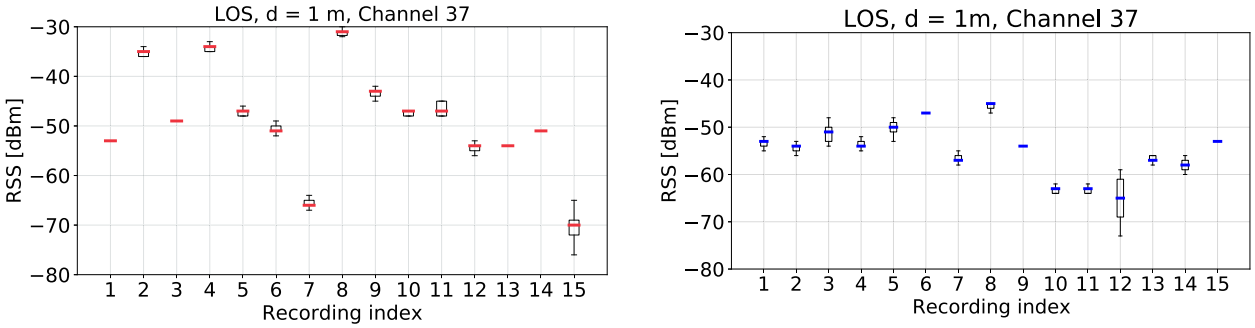

(a) UPB (b) TAU

Fig. 7. Boxplots showing the RSS distribution in 15 recordings acquired between the same device pair in LOS, at 1 m, at UPB and TAU, using only channel 37.

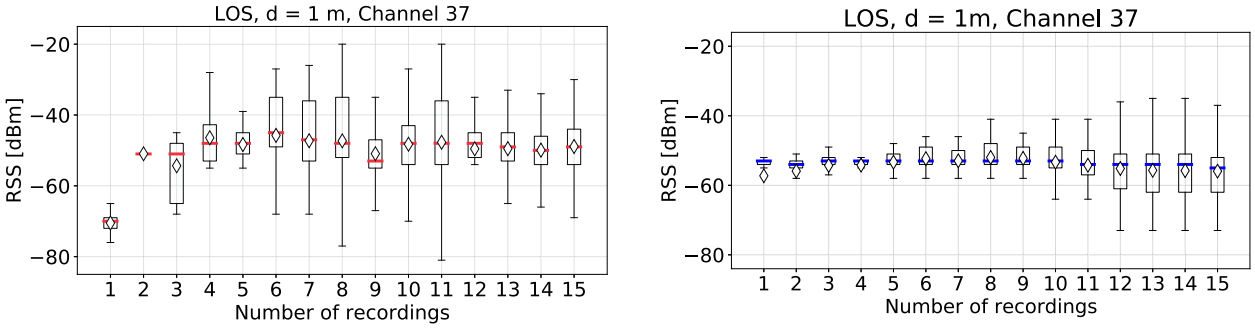

(a) UPB (b) TAU

Fig. 8. The impact of the number of snapshot recordings from a particular scenario on the RSS distribution. A total of 15 recordings were acquired in the same scenario (LOS at 1 m on channel 37). This figure presents the RSS distribution when an equal number of samples (326, corresponding to approximately 5 min) are taken from 1 to 15 recordings selected at random. The median, mean, and inter-quartile range (IQR) converge for more than 12–13 recordings.

in Section IV-A suggested that RSS measurements are very stable over time. For instance, recordings with indices 3, 4, and 5 were acquired at the exact same locations over multiple days but the mean RSS of recording number 4 is higher with 15 dB than the other two recordings. Such a large variability might be caused by the chipset warm-up after a reboot, interference in the ISM band, or other environmental factors such as the room temperature. Although we used the same model of devices for the measurements, the TAU data set from Fig. 7b had a smaller (but still significant) spread than the UPB data set from Fig. 7a, of 20 dB compared to 40 dB, respectively.

When aggregating data from multiple recordings, however, for at least 4 recordings the mean RSS converges to approximately −49 dBm and −55 dBm for UPB and TAU, respectively, as shown in Fig. 8. It is important to note that, although a relatively small number of recordings is necessary to capture the variability of the mean RSS between two devices across different locations, the shape of the distribution (and hence its spread) stabilizes only after 12–13 recordings.

C. The Impact of Hardware on the BLE RSS

We evaluated the impact of the hardware choice on the RSS when the same device model (Raspberry Pi 4 Model B) was used on both the transmitter and the receiver side. The devices were placed at the exact same location, with a fixed distance between them of 2 m, and the transmitter sent advertising beacons only on channel 37. We used in total four different Raspberry Pi boards, from exactly the same manufacturer and same model type, labeled `RPi1` to `RPi4` which integrate a Cypress CYW43455 BLE and Wi-Fi chipset.

Fig. 9 shows the RSS distribution of each pair of devices. Pair 1 consisted of the TX–RX pair `RPi1–RPi2`, pair 2 of `RPi1–RPi3`, pair 3 of `RPi1–RPi4`, pair 4 of `RPi2–RPi4`, and pair 5 of `RPi3–RPi4`. In other words, device pairs 1, 2, and 3 share the same transmitter, while device pairs 3, 4, and 5 share the same receiver. The median RSS varies with up to 5 dB even between devices from the same model. This experiment shows the difficulty of building a database that documents the transmitter and receiver efficiency of different brands of devices, since even devices that use the same hardware have RSS variations of several dB.

D. The Impact of the Advertising Channel Index on the BLE RSS

As mentioned earlier, BLE devices transmit beacons on channels 37, 38, and 39 which correspond to frequencies of 2.402, 2.426, and 2.48 GHz, respectively. Fig. 10 illustrates the impact of three advertising channels on the RSS, compared with a recording where all 3 advertising channels were used. The data was collected at the same location with the devices 2 m apart and on the same day within a short time interval. The same type of measurements were done in parallel at UPB

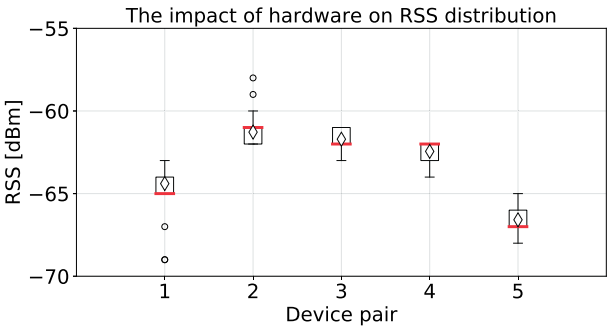

Fig. 9. The impact of hardware choice on the RSS in recordings acquired with different device pairs placed at a distance of 2 m at exactly the same location. The median RSS varies with 5 dB, even though the devices have the same model.

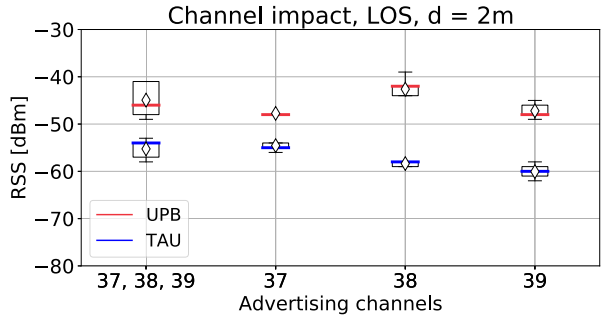

Fig. 10. The channel impact on RSS values in a LOS scenario at 2 m distance, based on measurements acquired at UPB and TAU. This plot illustrates the RSS distributions (with an equal number of samples: 95 per snapshot) when receiving beacons on all three channels and on individual channels.

and TAU. By default, beacons are transmitted on all three advertising channels. Therefore, a receiver cannot determine the channel of the transmitted packets, resulting in a larger variance of the samples and inaccurate distance estimates. At both UPB and TAU we noticed variations of at least 5 dB between measurements acquired on different channels. Other sources measured differences between BLE channels as high as 15 dB (Figure 2 in [54]).

E. The Impact of Transmitter-Receiver Distance on the BLE RSS

Under the LOS assumption (i.e., no obstacle between the a BLE transmitter and a receiver), one can start from the well-known free-space path-loss (FSL) model:

$$P_R = P_T - 20log_{10}d - 20log_{10}(\frac{4\pi f_c}{c}) + \eta, \quad (1)$$

where P_R is the received signal strength in dB scale, P_T is the apparent transmit power of the BLE transmitter computed at 1m away from the transmitter, d is the distance between the transmitter and the receiver (i.e., between the two persons under consideration in the digital contact-tracing app), f_c is the carrier frequency of the transmitted BLE signal (i.e., the carrier frequency on the used advertising channel or an average carrier frequency when several advertising channels are used), c is the speed of light (i.e., about $3 * 10^8$ m/s), and η is a noise factor encompassing the shadowing effects in the wireless channel, interference, and possible other noise sources. By virtue of the central-limit theorem, η can be assumed to be Gaussian distributed of variance σ^2. We also assume that η is a zero-mean noise under LOS scenarios.

The FSL is rarely used as such in RSS modeling; instead, most authors prefer the one-slope path-loss model below for its simplicity [27], [55]–[57]:

$$P_R = P_{T_a} - 10nlog_{10}d + \eta, \quad (2)$$

where the apparent transmit power P_{T_a} factor includes also the frequency-dependent effects, in such a way that multi-frequency effects, as those generated by RSS measurements on multiple advertising channels can be lumped into a single parameter, and n is a positive number modeling the path-loss parameter. An n value below the FSL path-loss factor of 2 would signal the presence of some conductivity effects in the building walls as well as multipath-enhanced propagation (e.g., multipath adding constructively). The lower n is, the flatter the RSS curve is with the distance, and the harder would be to differentiate between close distances (e.g., between 1m and 2 m or between 2 m and 3 m). Typically, in model-driven RSS approaches (as opposed to data-driven approaches), the purpose is to estimate the best-fit parameters P_{T_a} and n of an underlying path-loss model. This is usually done via a least-square (LS) fit, where the unknown parameter vector $\mathbf{x} \triangleq [P_{T_a}\ n]$ is estimated via $\hat{\mathbf{x}}$ [55]:

$$\hat{\mathbf{x}} = (\mathbf{A}^T\mathbf{A})^{-1}\mathbf{A}^T\mathbf{b}, \quad (3)$$

with $\mathbf{A} \in N_{meas} \times 2$ being a matrix with i-th row equal to $[1\ -10log_{10}d_i]$, $i = 1, \ldots, N_{meas}$, and $\mathbf{b} \in N_{meas} \times 1$ being a vector with the i-th element equal to the received signal strength P_{R_i} observed in the i-th measurement at d_i distance between TX and RX. Above, N_{meas} is the number of measurements (or observations) used in the LS fitting, and encompassing various TX-RX distances d_i. The shadowing variance $\hat{\sigma}_\eta^2$ is then computed as the error between the measurements and the reconstructed data, namely:

$$\hat{\sigma}_\eta^2 = \frac{1}{N_{meas}} \sum_{i=1}^{N_{meas}} \left(P_{R_i} - \hat{P}_{T_a} - 10\hat{n}log_{10}(d_i) \right)^2. \quad (4)$$

When a NLOS obstacle such as a glass window, a wall, or the body of another person is present between the transmitter and receiver, we expect the NLOS apparent transmit power P_{T_a} to be smaller than the LOS P_{T_a}, as it should incorporate the additional absorption losses due to obstacles. However, repeated measurements are both TAU and UPB showed that this is not always the case.

Table II gives examples of the path-loss parameters estimated from aggregated measurements on all three BLE advertising channel, in four considered scenarios (two LOS and two NLOS, with two of them from TAU and two from UPB scenarios). In the NLOS scenarios, the obstruction was caused by a wall between the TX and the RX. In order to have a fair comparison also between long recordings, we extracted 326 samples from each available recording (which correspond to a recording time of around 5 min) and aggregated them. Several

TABLE II
EXAMPLE OF PATH-LOSS PARAMETERS ESTIMATED FROM AGGREGATED MEASUREMENTS

Environment	$\hat{P}_{T_a}$ [dBm]	$\hat{n}$ [-]	$\hat{\sigma}_\eta$ [dB]	Total number of measurements		
				at 1 m	at 2 m	at 3 m
LOS, TAU	-55.35	0.76	6.01	5868	2608	1630
NLOS, TAU	-49.98	3.31	5.70	3586	2934	1956
LOS, UPB	-44.07	1.60	8.73	5216	2608	2934
NLOS, UPB	-51.69	0.37	8.72	1630	1630	1630

Monte Carlo runs showed very similar parameter-fit results from one run to another. For illustrative purposes, Table II shows the results based on one random run in each scenario.

The main conclusion is that there is not a one-size-fit-all model with constant $[\hat{P}_{T_a}\ \hat{n}]$ vector estimate, but that there are high fluctuations between the four shown scenarios, and therefore a model-driven approach for BLE RSS-based contact tracing will likely suffer from large errors. This is also reflected in the high shadowing standard deviations $\hat{\sigma}_\eta$ shown in Table II (around 6 dB for TAU data and around 9 dB for UPB data).

Indeed, other literature results have shown that the path-loss parameters used in different works vary widely. For instance, although a path-loss exponent between 2.4–2.6 is frequently recommended [26], in [43] the path-loss exponent was set to 1.8 for LOS scenarios and 2.2 for NLOS ones. In the survey part of [2], the path-loss exponents extracted from various research papers varied between 0.63–2.32 and TABLE II suggests that in some cases (NLOS, UPB) this value might be even lower.

Instead of model-driven contact tracing, data-driven approaches such as those based on large training data sets and machine learning solutions (e.g., in [26]) could be adopted, but they have high complexity and are impractical at large scales. Other works [58], [59] propose online path-loss estimation methods based on cooperating nodes in wireless sensor networks. However, tens of nodes are usually needed for an accurate estimation. Another solution is to have a gateway that collects the RSS of surrounding BLE beacons, tracks the fluctuations, and sends back RSS correction factors to individual nodes in real time [24]. However, such an approach is not suitable for a peer-to-peer and privacy-sensitive application like contact-tracing. Therefore, the challenges of finding the right approach (model-driven versus data-driven) and the right models (e.g., more sophisticated models than the simple single-slope path-loss model of Eq. (2)) are still important challenges to be solved by the research community dealing with BLE RSS-based contact tracing or proximity detection.

F. The Impact of Transmitter and Receiver Orientation on the BLE RSS

We considered the effect of the relative orientation between the transmitter and the receiver on the BLE RSS.

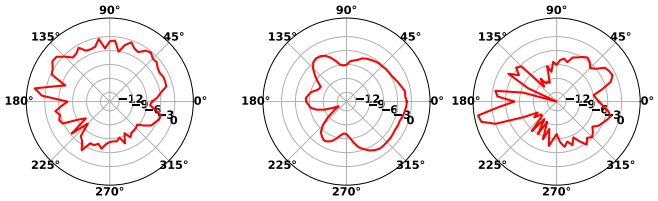

(a) Plane XY (b) Plane XZ (c) Plane YZ

Fig. 11. Radiation pattern of Raspberry Pi 3B+ antenna plotted from anechoic chamber measurement data [60]. It is a PCB antenna designed by Proant AB present in many IoT devices operating in the 2.4GHz band.

We analyzed four poses depicted in Fig. 12, where the pose of the transmitter is fixed and the receiver is rotated clock-wise with 90 °, 180 °, and 270 ° with respect to the "front" orientation from Fig. 12a, resulting in the "left," "right," and "back" poses, respectively. The radiation pattern (Fig. 11) for the frequency of Bluetooth channel 37 shows a 2.7 dB standard deviation across all angles, but the maximum differences on each of the three planes is of 10.1, 13, and 14.1 dB.

Fig. 13 presents the RSS distribution in all poses, when the devices are placed at distances of 1, 2, and 3 m. The devices were placed on tripods which were kept fixed at the aforementioned distances, while only the receiver was rotated around its center axis for each pose. Each recording had a duration of approximately 10 min and was performed only on channel 37. First, we notice the same inconsistencies with the distance discussed in Section IV-E, in which the average RSS at 1 m distance is lower than the one at 2 and 3 m. Second, the RSS changes with the pose for a particular distance, although the receiver was not moved but only rotated around its axis and the transmitter's position was the same in all recordings. There is no orientation which results in a higher RSS at all distances. However, the "back" pose has a lower median RSS than the other poses at all distances, most likely because in this pose, as can be seen from Fig. 12b, the metallic USB and Ethernet ports of the receiver board are in the LOS of the signal and attenuate it. While the median RSS in the "front," "left," and "right" poses varies with about 5 dB for the same distance, the median RSS in the "back" pose can be with even 20 dB lower than in the other poses.

G. Random Fluctuations Caused by BLE–Wi-Fi Combo Chipsets

The interference between Bluetooth and Wi-Fi is well documented in literature, and IEEE has recommendations [61] for the coexistence of the technologies operating in the ISM bands. [62] has shown experimentally that Bluetooth and ZigBee are affected by Wi-Fi, stating agreement with previous studies. One way to tackle the coexistence is to use specific algorithmic mitigations in the way each technology is used [63], but some might require updates to the standards. When both Wi-Fi and Bluetooth are implemented on the same chipset, as is the case with most smartphones, [64] determined through measurements that performance is degraded at the application layer.

For the purpose of contact tracing however, only RSS measurements and timestamps of the recordings are needed and

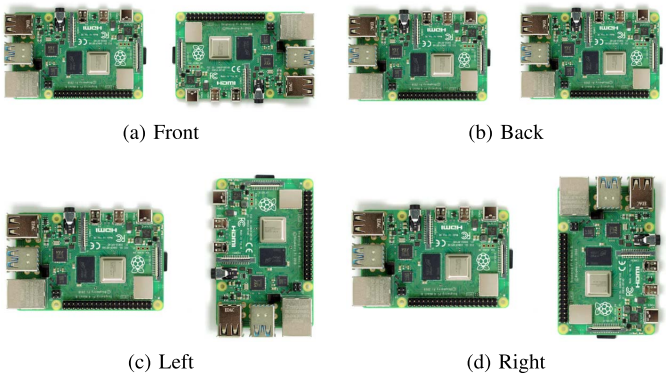

Fig. 12. The four orientations of the receiver (device on the right) with respect to the transmitter (device on the left) we considered in our experiment: (a) front, (b) back, (c) left, and (d) right. In the back, left, and right poses the receiver was rotated clock-wise with, respectively, 180°, 90°, and 270° with respect to the front orientation.

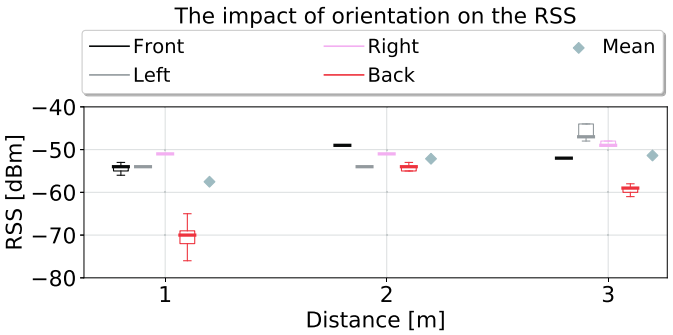

Fig. 13. The impact of orientation on the BLE RSS. The front, left, right, and back orientations are shown in Fig. 12.

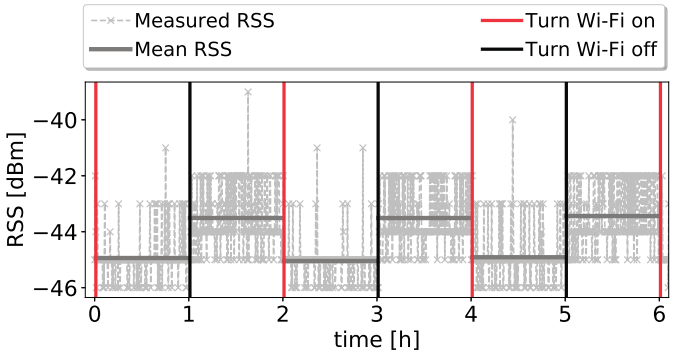

Fig. 14. The impact of Wi-Fi and BLE combo chipsets: the Wi-Fi is turned on and off every one hour at the indicated markers. On average, the mean RSS with the Wi-Fi off is with 2.5 dB higher than with the Wi-Fi off.

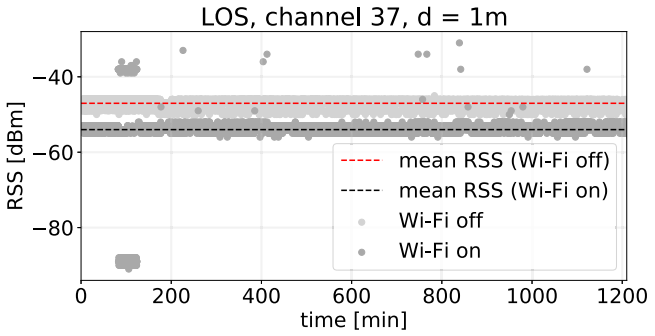

Fig. 15. The impact of Wi-Fi switched on and off, in LOS at 1m distance. When the Wi-Fi is off, the mean RSS is higher with 6.8 dB than when the Wi-Fi is on. When the Wi-Fi is on, we also notice RSS fluctuations of up to 30 dB around minute 100.

the question is whether the BLE measurements are influenced by Wi-Fi activity on the same chipset. We turn the Wi-Fi on and off simultaneously at both the transmitter and the receiver every one hour and record the RSS. During the time when the Wi-Fi is on, synthetic Wi-Fi traffic is generated with 112 kb/s. Fig. 14 shows that, on average, the mean RSS when the Wi-Fi is on is 2.5 dB lower than during the time the Wi-Fi is off. There is also a small difference in the standard deviation: when the Wi-Fi is on, the standard deviation of the RSS is 1.1 dB compared to 0.83 dB when the Wi-Fi is off. Although Fig. 14 presents the results for 6 hours only, for better visualization, the pattern remained consistent over two days, during which there was no human activity around the devices.

Wi-Fi scanning might occasionally cause even larger differences in the BLE RSS than 2.5 dB. We sometimes noticed spurious measurements occurring only when the Wi-Fi was on, usually at the beginning of a snapshot recording, as shown in Fig. 15 around minute 100, when the signal fluctuated for several minutes between −40, −55, and −90 dB. The recordings with the settings of Wi-Fi on and off were acquired during different times of the day; however, the environment was static with no people moving inside the room. We acquired results which show the mean RSS values to be with 6.8 dB higher with Wi-Fi off than with Wi-Fi switched on. Overall, Fig. 15 illustrates the instabilities in single recordings which might be caused by coexistence of different signals within the 2.4 GHz frequency. A similar pattern was observed also in [65], where Figures 6 and 7 reveal a 20 dB difference in BLE readings when Wi-Fi scanning is active with a Samsung Galaxy S4 smartphone.

H. On the Difficulty of LOS/NLOS Detection

In this section, we investigate the effect of different types of obstructions on the BLE RSS. At both UPB and TAU we acquired measurements in LOS and NLOS with wall shadowing. In addition, at UPB, we tried more types of obstructions: wall and whiteboard, door, human body, and plexiglass panel. All the setups are shown in Fig. 4, where for NLOS measurements we varied only the distance between the devices, while in LOS we also tried different locations.

We consider a "scenario" a set of snapshot measurements acquired at the same distance, on the same channel, in the same LOS/NLOS setting. TABLE III presents the mean and the standard deviation of the RSS computed in different scenarios from measurements acquired at UPB. Because recordings in the same scenarios have lengths from 5 min to several days and we do not want longer recordings to bias the statistics, when there are multiple recordings in the same scenario we chose an equal number of measurements at random from each

recording from that scenario and computed the mean and standard deviation using only the subset of samples. Usually, recordings within the same scenario were acquired at different locations to capture the variability of the RSS across space for the same TX–RX distance. As a result, when there are multiple recordings in a scenario, the standard deviation of the RSS is higher than in single-recording scenarios. The number of recordings ("Nr. rec.") and the number of samples in each recording ("Nr. samples per rec.") are specified in TABLE III for each scenario, as well as the advertising channel(s) on which measurements were acquired.

Comparing the statistics in LOS and NLOS when all advertising channels are used, we note that the mean RSS varies within a range of 20 dB, indicating that the attenuation introduced by an obstacle depends on the type of obstacle. The mean RSS in LOS is usually higher than the one in NLOS but not always—the mean RSS in the "NLOS door" recording is higher than the one in LOS. Note also that the human body causes a higher standard deviation than the other obstructions. This can be seen more clearly in Fig. 16, which shows the distributions of selected NLOS measurements from TABLE III and one recording acquired in LOS on all channels. The large spread can be caused by slight movements of the body which, by nature, cannot be perfectly immobile (breathing alone causes a slight movement of the body). These characteristics can make the human body more easily detectable than other obstructions, as previous works showed [26]. However, other obstructions might be more difficult to detect. For instance, the mean RSS in the "NLOS plexiglass" case is similar to the mean RSS in LOS on individual channels, while the highest mean RSS was obtained in the "NLOS door" case.

The inconsistency can be also caused by the fact that most of the NLOS statistics were computed based on a single recording and, as we saw in Section IV-B, single recordings can deviate from statistics computed on aggregated data with more than 10 dB. Therefore, next we compare LOS and NLOS with a wall distributions aggregated from all channels, at distances of 1, 2, and 3 m, acquired independently at UPB and TAU, shown in Fig. 17. The distributions are plotted based on the same data used in Section IV-E to estimate the path-loss parameters from TABLE II. Each distribution was computed based on 5 to 18 recordings based on 326 measurements selected at random from each recording. Based on the results in Section IV-B, the mean computed based on 5 recordings should be within several dB of the "stable" mean, but the standard deviation can still fluctuate for less than 12–13 recordings.

Although the distributions in Fig. 17 mostly behave as expected, i.e. the mean RSS should decrease with the distance and the mean RSS should be lower in NLOS than in LOS at the same distance, there are exceptions. The average RSS in NLOS is higher than the one in LOS at 3 m for the UPB data set and at 1 m for the TAU data set. Also, the NLOS distributions have higher or equal spread than LOS ones in most of the cases, even though the NLOS data sets contained less recordings than the LOS ones. This result contradicts observations in [43], where NLOS obstructions caused by walls were identified when the standard deviation of RSS measurements in a window was *lower* than a fixed threshold.

TABLE III
THE MEAN AND STANDARD DEVIATION OF THE BLE RSS IN DIFFERENT SCENARIOS AT A TX–RX DISTANCE OF 2 m

Scenario	Ch.	Nr. rec.	Nr. samples per rec.	RSS	
				Mean [dBm]	Std. [dB]
LOS	37	7	326	−50.5	7.6
LOS	38	1	3215	−46.0	5.6
LOS	39	1	25 607	−54.2	1.7
LOS	all	5	736	−45.6	7.3
NLOS wall	37	3	1726	−55.4	6.0
NLOS wall	all	1	1824	−58.2	2.0
NLOS human	all	1	495	−60.0	4.3
NLOS plexiglass	all	1	1824	−50.7	2.9
NLOS door	all	1	1808	−40.7	3.3

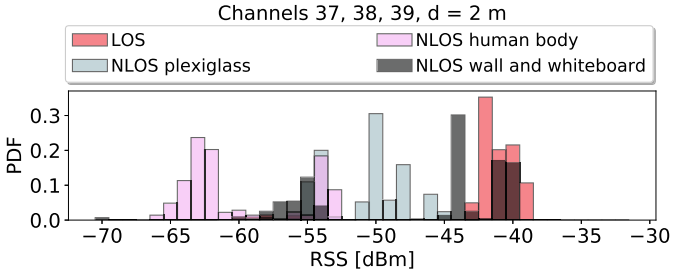

Fig. 16. Comparison of selected RSS distributions acquired on all advertising channels at 2 m, in LOS, NLOS with a plexiglass panel, NLOS with a wall and a whiteboard, and NLOS with human body shadowing.

Although UPB and TAU data sets were acquired using the same model of Raspberry Pis, measurements acquired at TAU had a smaller spread than those from UPB even in LOS, which points once more to the instability of RSS measurements.

In proximity-detection or RSS-based localization applications, obstructions will most of the time lead to inaccurate distance or location estimates. Therefore, multiple solutions have been proposed to correct RSS-based ranges by detecting the NLOS condition [26], [42], [43] with the caveat that such solutions might not generalize easily, as our measurements show, or that large data sets might be necessary to extract features that improve classification. In contact-tracing applications, such instabilities can lead to false alarms or failures in detecting potentially unsafe interactions. For instance, since human body shadowing sharply attenuates the signal, the distance predicted by a standard path-loss model can be larger than in reality, so people might not be notified of risky encounters. On the contrary, if the RSS reported when devices (or people) are separated by walls is larger or equal than the average RSS in LOS, an alert might be raised even if people staying in different rooms are safe from each other. Therefore, LOS/NLOS detection is still a highly relevant topic with room for improvement. Hybrid solutions that combine BLE with UWB, cameras, or other sensors might increase the reliability of NLOS detection.

V. DISCUSSION

One of the unexpected results of our measurement campaigns—a result which has also not been emphasized

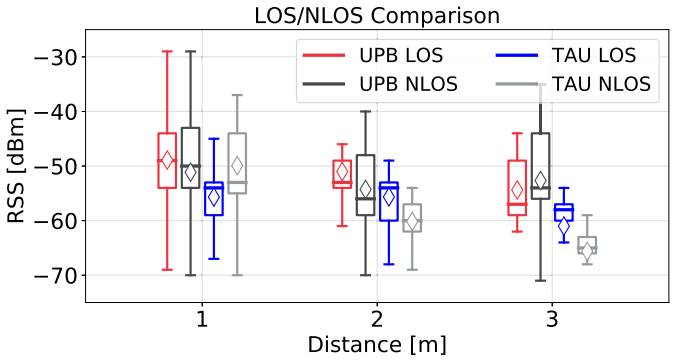

Fig. 17. Comparison of RSS distributions based on data acquired in LOS and NLOS with a wall at UPB and TAU at distances of 1, 2, and 3 m, irrespective of the advertisement channel.

enough until now in the current literature—is the fact that snapshot BLE RSS measurements are highly unstable and fluctuating, and only by lumping together enough measurements (i.e., by using aggregated data), the results seem to converge, to some extent, to the classical path-loss models (e.g., average RSS decreasing with transmitter-receiver distances, average RSS under LOS scenarios stronger than the average RSS under NLOS scenarios). Nevertheless, for fast proximity-detection or contact-tracing algorithms, when the observation window can be as small as 15 min, aggregated RSS data may be unavailable, and estimations based on what we called snapshot recordings can suffer from significant errors due to high RSS fluctuations. We also provided guidelines for building data sets that best represent the conditions in a particular scenario.

VI. Conclusion, and Open Issues

This paper presented a detailed analysis of BLE RSS fluctuations based on an extensive measurement campaign performed in tandem in Tampere, Finland, and Bucharest, Romania. We documented in detail the main sources of high fluctuations (or instabilities) of BLE RSS measurements occurring, surprisingly, in static scenarios and diverging from the classical path-loss models, e.g., as given in Eqs. (1) and (2). We defined controlled scenarios, such as fixing the transmitter and receiver BLE models, fixing the BLE advertising channel to have transmission on a single carrier frequency, turning the Wi-Fi transmitter off in chipsets sharing the 2.4 GHz antenna between BLE and Wi-Fi, and fixing the transmitter-receiver distance.

We emphasized several challenges that still remain to be addressed by the research community when standalone BLE RSS measurements are used for contact tracing, proximity detection, or positioning purposes, namely: the challenges of NLOS scenarios with stronger average (and median) RSS than LOS scenarios at the same distance, the challenge of increased RSS fluctuations (or variance) when the measurements are acquired on multiple BLE advertising channels (as it is customary in contact-tracing applications) or with different receiver-transmitter orientations (which again are highly variable, as users can keep their mobile devices in various positions: in hand, inside bags, inside front or back pockets, etc.).

A possible solution to overcome the instability of snapshot BLE RSS recordings is, for example, the hybridization of BLE RSS measurements with other sensors, such as vision sensors (to enable LOS/NLOS detection) or time-of-arrival UWB sensors (to enhance the range estimation). However, this will increase the energy consumption of end-user devices, so the trade-off between proximity detection accuracy and energy consumption must also be considered. Collecting data from additional sensors can also potentially decrease user privacy. Another possibility would be to collect large training databases in hotspot areas (e.g., shopping centers, commuting halls, etc.), which could facilitate a baseline statistical modeling based on both snapshot and aggregated training data, and to further use machine-learning approaches to derive data-driven estimators instead of the model-driven estimators which rely on path-loss modeling.

The main goal of this paper is to shed additional light on the challenges encountered in BLE-based contact tracing and to raise awareness among the research community that several challenges related to BLE RSS ranging and positioning are still to be solved. One solution based on our measurements is to use enough aggregated data, as, by virtue of the central-limit theorem, this seems to remove the outliers and to converge towards known path-loss models. Such a solution could be sufficient for positioning purposes when training databases can be based on large amounts of aggregated data, but it may still be unfeasible for contact-tracing solutions in need working with snapshot data. Another solution could envisage more sophisticated path-loss modeling, such as by taking waveguide effects [66] into account or using stochastic ray-tracing modeling [67].

The measurement data will be made open-access at the research community on Zenodo,[2] in order to enable the reproducibility of the research and to provide benchmark data for further investigations on BLE RSS-based contact tracing. Future work also includes collecting data from more devices, including various types of mobile phones, and looking into more detail at the yet-unsolved research question of whether NLOS situations can be separated with high accuracy from LOS situations and under which conditions.

References

[1] V. Shubina, S. Holcer, M. Gould, and E. S. Lohan, "Survey of decentralized solutions with mobile devices for user location tracking, proximity detection, and contact tracing in the COVID-19 era," *Data*, vol. 5, no. 4, p. 87, Sep. 2020.

[2] V. Shubina, A. Ometov, A. Basiri, and E. S. Lohan, "Effectiveness modelling of digital contact-tracing solutions for tackling the COVID-19 pandemic," *J. Navigat.*, vol. 4, pp. 1–37, Apr. 2021.

[3] C. T. Nguyen *et al.*, "A comprehensive survey of enabling and emerging technologies for social distancing—Part I: Fundamentals and enabling technologies," *IEEE Access*, vol. 8, pp. 153479–153507, 2020.

[4] C. T. Nguyen *et al.*, "A comprehensive survey of enabling and emerging technologies for social distancing—Part II: Emerging technologies and open issues," *IEEE Access*, vol. 8, pp. 154209–154236, 2020.

[5] E. Hernandez-Orallo, P. Manzoni, C. T. Calafate, and J.-C. Cano, "Evaluating how smartphone contact tracing technology can reduce the spread of infectious diseases: The case of COVID-19," *IEEE Access*, vol. 8, pp. 99083–99097, 2020.

[6] I. Braithwaite, T. Callender, M. Bullock, and R. W. Aldridge, "Automated and partly automated contact tracing: A systematic review to inform the control of COVID-19," *Lancet Digit. Health*, vol. 2, no. 11, pp. e607–e621, Nov. 2020.

[7] N. Ahmed *et al.*, "A survey of COVID-19 contact tracing apps," *IEEE Access*, vol. 8, pp. 134577–134601, 2020.

[2] https://doi.org/10.5281/zenodo.4643668

[8] A. Basiri *et al.*, "Indoor location based services challenges, requirements and usability of current solutions," *Comput. Sci. Rev.*, vol. 24, pp. 1–12, May 2017.

[9] S. Tomic, M. Beko, R. Dinis, M. Tuba, and N. Bacanin, "Bayesian methodology for target tracking using combined RSS and AoA measurements," *Phys. Commun.*, vol. 25, pp. 158–166, Dec. 2017.

[10] F. Della Rosa, T. Paakki, J. Nurmi, and M. Pelosi, "Exploiting RSS measurements among neighbouring devices: A matter of trust," in *Proc. Int. Conf. Indoor Positioning Indoor Navigat.*, Oct. 2013, pp. 1–8.

[11] C. Gentner, D. Günther, and P. H. Kindt, "Identifying the BLE advertising channel for reliable distance estimation on smartphones," 2020, *arXiv:2006.09099*. [Online]. Available: https://arxiv.org/abs/2006.09099

[12] A. Kara and H. L. Bertoni, "Blockage/shadowing and polarization measurements at 2.45 GHz for interference evaluation between Bluetooth and IEEE 802.11 WLAN," in *Proc. IEEE Antennas Propag. Soc. Int. Symp., Dig. Held Conjunction, USNC/URSI Nat. Radio Sci. Meeting*, Boston, MA, USA, vol. 3, Jul. 2001, pp. 376–379.

[13] U. M. Qureshi, Z. Umair, Y. Duan, and G. P. Hancke, "Analysis of Bluetooth low energy (BLE) based indoor localization system with multiple transmission power levels," in *Proc. IEEE 27th Int. Symp. Ind. Electron. (ISIE)*, Jun. 2018, pp. 1302–1307.

[14] Y. Li, Z. He, Y. Li, Z. Gao, R. Chen, and N. El-Sheimy, "Enhanced wireless localization based on orientation-compensation model and differential received signal strength," *IEEE Sensors J.*, vol. 19, no. 11, pp. 4201–4210, Jun. 2019.

[15] F. Della Rosa, T. Paakki, J. Nurmi, M. Pelosi, and G. D. Rosa, "Handgrip impact on range-based cooperative positioning," in *Proc. 11th Int. Symp. Wireless Commun. Syst. (ISWCS)*, 2014, pp. 728–732.

[16] P. Handayani, L. Mubarokah, and G. Hendrantoro, "Pathloss and shadowing characteristics in indoor environment at 2.4 GHz band," in *Proc. Int. Seminar Intell. Technol. Appl. (ISITIA)*, pp. 423–428, 2015.

[17] C. Xiang *et al.*, "CARM: Crowd-sensing accurate outdoor RSS maps with error-prone smartphone measurements," *IEEE Trans. Mobile Comput.*, vol. 15, no. 11, pp. 2669–2681, Nov. 2016.

[18] Q. Wang, D. W. Matolak, and B. Ai, "Shadowing characterization for 5-GHz vehicle-to-vehicle channels," *IEEE Trans. Veh. Technol.*, vol. 67, no. 3, pp. 1855–1866, Mar. 2018.

[19] M. Sasaki, T. Nakahira, K. Wakao, and T. Moriyama, "Human blockage loss characteristics of 5 GHz Wi-Fi band in a crowded stadium," *IEEE Antennas Wireless Propag. Lett.*, vol. 20, no. 6, pp. 988–992, Jun. 2021.

[20] MIT. *PACT Datasets and Evaluation*. Accessed: Jun. 24, 2021. [Online]. Available: https://github.com/mitll/BLE-RSSI-Various-Static-Configurations

[21] C. Li and L. Shi. *Exposure Notification (Contact Tracing) System on Raspberry Pi*. Accessed: Jun. 24, 2021. [Online]. Available: https://github.com/ececli/Exposure-Notification-on-RPi

[22] L. Trommer and N. Kühnapfel. *Test of COVID-19 Bluetooth LE Localization Precision*. Accessed: Jun. 24, 2021. [Online]. Available: https://github.com/niclasku/ble-distance-measurements

[23] *A Technical Roadmap for the UK's Contact Tracing APP Functionality*. Accessed: Mar. 31, 2021. [Online]. Available: https://www.turing.ac.uk/blog/technical-roadmap-uks-contract-tracing-app-functionality

[24] A. Nikoukar, M. Abboud, B. Samadi, M. Gunes, and B. Dezfouli, "Empirical analysis and modeling of Bluetooth low-energy (BLE) advertisement channels," in *Proc. 17th Annu. Medit. Ad Hoc Netw. Workshop (Med-Hoc-Net)*, Jun. 2018, pp. 1–6.

[25] R. Faragher and R. Harle, "Location fingerprinting with Bluetooth low energy beacons," *IEEE J. Sel. Areas Commun.*, vol. 33, no. 11, pp. 2418–2428, Nov. 2015.

[26] S. Naghdi and K. O'Keefe, "Detecting and correcting for human obstacles in BLE trilateration using artificial intelligence," *Sensors*, vol. 20, no. 5, p. 1350, Feb. 2020.

[27] E. S. Lohan, J. Talvitie, P. Figueiredo e Silva, H. Nurminen, S. Ali-Loytty, and R. Piche, "Received signal strength models for WLAN and BLE-based indoor positioning in multi-floor buildings," in *Proc. Int. Conf. Location GNSS (ICL-GNSS)*, Jun. 2015, pp. 1–6.

[28] J. Neburka *et al.*, "Study of the performance of RSSI based Bluetooth smart indoor positioning," in *Proc. 26th Int. Conf. Radioelektronika (RADIOELEKTRONIKA)*, Apr. 2016, pp. 121–125.

[29] G. De Blasio, A. Quesada-Arencibia, C. R. Garcia, J. C. Rodriguez-Rodriguez, and R. Moreno-Diaz, "A protocol-channel-based indoor positioning performance study for Bluetooth low energy," *IEEE Access*, vol. 6, pp. 33440–33450, 2018.

[30] D. Sikeridis, I. Papapanagiotou, and M. Devetsikiotis, "BLEBeacon: A real-subject trial dataset from mobile Bluetooth low energy beacons," 2018, *arXiv:1802.08782*. [Online]. Available: http://arxiv.org/abs/1802.08782

[31] N. Mohsin, S. Payandeh, D. Ho, and J. P. Gelinas, "Study of activity tracking through Bluetooth low energy-based network," *J. Sensors*, vol. 2019, p. 6876925, Feb. 2019.

[32] G. M. Mendoza-Silva, M. Matey-Sanz, J. Torres-Sospedra, and J. Huerta, "BLE RSS measurements dataset for research on accurate indoor positioning," *Data*, vol. 4, no. 1, p. 12, 2019.

[33] P. Chet Ng, P. Spachos, and K. Plataniotis, "COVID-19 and your smartphone: BLE-based smart contact tracing," 2020, *arXiv:2005.13754*. [Online]. Available: http://arxiv.org/abs/2005.13754

[34] D. J. Leith and S. Farrell, "Coronavirus contact tracing: Evaluating the potential of using Bluetooth received signal strength for proximity detection," *ACM SIGCOMM Comput. Commun. Rev.*, vol. 50, no. 4, pp. 66–74, 2020.

[35] S. Sadowski, P. Spachos, and K. N. Plataniotis, "Memoryless techniques and wireless technologies for indoor localization with the Internet of Things," *IEEE Internet Things J.*, vol. 7, no. 11, pp. 10996–11005, 2020.

[36] P. C. Ng, P. Spachos, and K. N. Plataniotis, "COVID-19 and your smartphone: BLE-based smart contact tracing," *IEEE Syst. J.*, early access, Mar. 9, 2021, doi: 10.1109/JSYST.2021.3055675.

[37] A. F. Molisch, *Wireless Communication*, vol. 34. Hoboken, NJ, USA: Wiley, 2012.

[38] J. Paek, J. Ko, and H. Shin, "A measurement study of ble ibeacon and geometric adjustment scheme for indoor location-based mobile applications," *Mobile Inf. Syst.*, vol. 2016, Oct. 2016, Art. no. 8367638.

[39] M. Castillo-Cara, J. Lovón-Melgarejo, G. Bravo-Rocca, L. Orozco-Barbosa, and I. García-Varea, "An empirical study of the transmission power setting for Bluetooth-based indoor localization mechanisms," *Sensors*, vol. 17, no. 6, p. 1318, 2017.

[40] *Exposure Notifications BLE Calibration Calculation*. Accessed: Mar. 31, 2021. [Online]. Available: https://developers.google.com/android/exposure-notifications/ble-attenuation-computation#rssi-tx-power

[41] *Android Fragmentation Visualized*. Accessed: Mar. 31, 2021. [Online]. Available: https://www.opensignal.com/sites/opensignal-com/files/data/reports/global/data-2015-08/2015_08_fragmentation_report.pdf

[42] G. de Blasio, A. Quesada-Arencibia, C. García, J. Molina-Gil, and C. Caballero-Gil, "Study on an indoor positioning system for harsh environments based on Wi-Fi and Bluetooth low energy," *Sensors*, vol. 17, no. 6, p. 1299, Jun. 2017.

[43] A. A. Juri, T. Arslan, and F. Wang, "Obstruction-aware Bluetooth low energy indoor positioning," in *Proc. 29th Int. Tech. Meeting The Satell. Division Inst. Navigat.*, pp. 2254–2261, 2016.

[44] M. Youssef, M. Mah, and A. Agrawala, "Challenges: Device-free passive localization for wireless environments," in *Proc. 13th Annu. ACM Int. Conf. Mobile Comput. Netw.*, 2007, pp. 222–229.

[45] K. Woyach, D. Puccinelli, and M. Haenggi, "Sensorless sensing in wireless networks: Implementation and measurements," in *Proc. 4th Int. Symp. Model. Optim. Mobile, Ad Hoc Wireless Netw.*, 2006, pp. 1–8.

[46] N. Fet, M. Handte, and P. J. Marrón, "A model for wlan signal attenuation of the human body," in *Proc. ACM Int. joint Conf. Pervas. Ubiquitous Comput.*, 2013, pp. 499–508.

[47] S. Galmiche *et al.*, "Exposures associated with SARS-CoV-2 infection in france: A nationwide online case-control study," *Lancet Regional Health*, vol. 7, Aug. 2021, Art. no. 100148.

[48] T. C. Bulfone, M. Malekinejad, G. W. Rutherford, and N. Razani, "Outdoor transmission of SARS-CoV-2 and other respiratory viruses: A systematic review," *J. Infectious Diseases*, vol. 223, pp. 550–561, Nov. 2020.

[49] D. Niculescu, "Interference map for 802.11 networks," in *Proc. 7th ACM SIGCOMM Conf. Internet Meas.*, 2007, pp. 339–350.

[50] Y. Chapre, P. Mohapatra, S. Jha, and A. Seneviratne, "Received signal strength indicator and its analysis in a typical wlan system (short paper)," in *Proc. 38th Annu. Conf. Local Comput. Netw.*, 2013, pp. 304–307. [Online]. Available: https://ieeexplore.ieee.org/abstract/document/6761255?casa_token=LzstcJu3likAAAAA:lT5mHlM6DHFaL-5XiVMiTTIswDr92UgDNOgGR4DCwz8p5xkM6952MkLhVecd6EW3lX3Dkt28KLV3

[51] D. Lymberopoulos, Q. Lindsey, and A. Savvides, "An empirical characterization of radio signal strength variability in 3-D IEEE 802.15. 4 networks using monopole antennas," in *Proc. Eur. Workshop Wireless Sensor Netw.* Springer, 2006, pp. 326–341.

[52] *Exposure Notification Bluetooth Specification, Version 1.2*. Accessed: Mar. 31, 2021. [Online]. Available: https://covid19-static.cdn-apple.com/applications/covid19/current/static/contact-tracing/pdf/ExposureNotification-BluetoothSpecificationv1.2.pdf

[53] D. J. Leith and S. Farrell, "Gaen due diligence: Verifying the Google/Apple COVID exposure notification API," in *Proc. NDSS*, 2021, pp. 1–5.
[54] J. Powar, C. Gao, and R. Harle, "Assessing the impact of multi-channel ble beacons on fingerprint-based positioning," in *Proc. Int. Conf. Indoor Positioning Indoor Navigat. (IPIN)*, Apr. 2017, pp. 1–8.
[55] S. Shrestha, J. Talvitie, and E. S. Lohan, "Deconvolution-based indoor localization with wlan signals and unknown access point locations," in *Proc. Int. Conf. Localization GNSS (ICL-GNSS)*, 2013, pp. 1–6.
[56] A. Zanella, "Best practice in RSS measurements and ranging," *IEEE Commun. Surveys Tuts.*, vol. 18, no. 4, pp. 2662–2686, 4th Quart., 2016.
[57] Z. He, Y. Li, L. Pei, R. Chen, and N. El-Sheimy, "Calibrating multi-channel RSS observations for localization using Gaussian process," *IEEE Wireless Commun. Lett.*, vol. 8, no. 4, pp. 1116–1119, Jun. 2019.
[58] A. Bel, J. L. Vicario, and G. Seco-Granados, "Localization algorithm with on-line path loss estimation and node selection," *Sensors*, vol. 11, no. 7, pp. 6905–6925, Jul. 2011.
[59] G. Mao, B. D. O. Anderson, and B. Fidan, "Path loss exponent estimation for wireless sensor network localization," *Comput. Netw.*, vol. 51, no. 10, pp. 2467–2483, Jul. 2007.
[60] ATL Company. *Raspberry Pi Model 3B+ Antenna Evaluation*. Accessed: Mar. 31, 2021. [Online]. Available: https://antennatestlab.com/antenna-examples/raspberry-pi-model-3b-antenna-evaluation-gain-pattern
[61] L. M. S. Committee *et al.*, "Coexistence of wireless personal area networks with other wireless devices operating in unlicensed frequency bands," *IEEE Comput. Soc.*, vol. 425, p. 429, Aug. 2003.
[62] R. G. Garroppo, L. Gazzarrini, S. Giordano, and L. Tavanti, "Experimental assessment of the coexistence of Wi-Fi, ZigBee, and Bluetooth devices," in *Proc. IEEE Int. Symp. World Wireless, Mobile Multimedia Netw.*, 2011, pp. 1–9.
[63] N. Golmie, N. Chevrollier, and O. Rebala, "Bluetooth and WLAN coexistence: Challenges and solutions," *IEEE Wireless Commun.*, vol. 10, no. 6, pp. 22–29, Dec. 2003.
[64] R. Friedman, A. Kogan, and Y. Krivolapov, "On power and throughput tradeoffs of WiFi and Bluetooth in smartphones," *IEEE Trans. Mobile Comput.*, vol. 12, no. 7, pp. 1363–1376, Jul. 2013.
[65] R. Faragher and R. Harle, "An analysis of the accuracy of Bluetooth low energy for indoor positioning applications," in *Proc. 27th Int. Tech. Meeting The Satell. Division Inst. Navigat. (ION GNSS+ 2014)*, 2014, pp. 201–210.
[66] K. Park, J. Lee, S. Hyun, and S. Kim, "Analysis of path loss properties in indoor hallway with waveguide channel model," in *Proc. IEEE VTS Asia Pacific Wireless Commun. Symp. (APWCS)*, Aug. 2019, pp. 1–5.
[67] T. Zwick, C. Fischer, D. Didascalou, and W. Wiesbeck, "A stochastic spatial channel model based on wave-propagation modeling," *IEEE J. Sel. Areas Commun.*, vol. 18, no. 1, pp. 6–15, Jan. 2000.

Laura Flueratoru (Graduate Student Member, IEEE) received the B.Eng. degree in electronics and telecommunications from the University Politehnica of Bucharest, Romania, in 2017, and the M.Sc. degree in electrical engineering from ETH Zürich, Switzerland, in 2019. She is currently pursuing the dual Ph.D. degree with the University Politehnica of Bucharest, and Tampere University, Finland, as a Marie Skłodowska-Curie Fellow in the European project A-WEAR. During her studies, she gained experience in industry and research from internships at Freescale Semiconductor, École Polytechnique Fédérale de Lausanne (EPFL), and Schindler Group. Her research interests include indoor localization, wireless and mobile communications, embedded systems, signal processing, and machine learning.

Viktoriia Shubina (Graduate Student Member, IEEE) received the M.Sc. degree in engineering from the University of Applied Sciences Technikum Wien, Austria, and the M.Sc. degree in business informatics from the National Research University Higher School of Economics, Russia, in 2019. She is pursuing the dual Ph.D. degree with Tampere University, Finland, and the University Politehnica of Bucharest, Romania. She is an Early-Stage Researcher with the EU Horizon 2020 Marie Skłodowska-Curie Project A-WEAR. Her research interests include indoor positioning, privacy-aware localization, and privacy-preserving mechanisms.

Dragoş Niculescu received the Ph.D. degree in computer science from Rutgers University, New Jersey, in 2004, with a thesis on sensor networks routing and positioning. He spent five years as a Researcher with NEC Laboratories America, Princeton, NJ, USA, working on simulation and implementation of mesh networks, VoIP, and WiFi-related protocols. At University Politehnica of Bucharest, he is currently teaching courses in mobile computing and services for mobile networking; also researching mobile protocols, UWB, and 802.11 networking.

Elena Simona Lohan (Senior Member, IEEE) received the M.Sc. degree in electrical engineering from the Polytechnics University of Bucharest in 1997, the D.E.A. degree in econometrics with the Ecole Polytechnique, Paris, in 1998, and the Ph.D. degree in telecommunications from the Tampere University of Technology in 2003. She is a Full Professor with the Electrical Engineering Unit, Tampere University (TAU) and a Visiting Professor with the Universitat Autonoma de Barcelona (UAB), Spain. She is leading a Research Group on signal processing for wireless positioning. She is the author or coauthor in more than 220 international peer-reviewed publications, six patents, and inventions. She is also coordinating the A-WEAR MSCA European Joint Doctorate Network in the field of wearable computing. Her research interests include signal processing for wireless positioning and navigation, multipath and interference mitigation, and RF fingerprinting. She is a Co-Editor of the first book on Galileo satellite system *Galileo Positioning Technology* (Springer) and a Co-Editor of a Springer book on *Multi-Technology Positioning*. She is also an Associate Editor of *RIN Journal of Navigation* and *IET Journal on Radar, Sonar, and Navigation*.